High-Fidelity Quantum Logic Gates Using Trapped-Ion Hyperfine Qubits

C. J. Ballance, T. P. Harty, N. M. Linke, M. A. Sepiol, and D. M. Lucas

Phys. Rev. Lett. **117**, 060504 — Published 4 August 2016

DOI: 10.1103/PhysRevLett.117.060504

High-fidelity quantum logic gates using trapped-ion hyperfine qubits

C. J. Ballance, T. P. Harty, N. M. Linke, M. A. Sepiol and D. M. Lucas*
Department of Physics, University of Oxford, Clarendon Laboratory, Parks Road, Oxford OX1 3PU, U.K.
(Dated: 21 June 2016, v10.2)

We demonstrate laser-driven two-qubit and single-qubit logic gates with fidelities 99.9(1)% and 99.9934(3)% respectively, significantly above the $\approx 99\%$ minimum threshold level required for fault-tolerant quantum computation, using qubits stored in hyperfine ground states of calcium-43 ions held in a room-temperature trap. We study the speed/fidelity trade-off for the two-qubit gate, for gate times between 3.8 μs and 520 μs, and develop a theoretical error model which is consistent with the data and which allows us to identify the principal technical sources of infidelity.

A powerful quantum computer need not require more than a few thousand logical qubits, but the number of physical qubits required depends strongly on the precision with which they can be manipulated [1]. Fault-tolerant quantum error correction typically requires that the errors associated with all operations (qubit initialization, single- and two-qubit logic gates, and readout) must each be below a threshold level of $\approx 1\%$ in order for a quantum computer to function at all [2–4]. The ability to entangle qubits "on demand" has been demonstrated in several physical systems [5–8] and error rates slightly below threshold have been achieved using trapped ions [9] and superconducting circuits [10]. However, the precision has so far fallen short of that needed for the construction of a practical quantum computer, because error rates at least an order of magnitude below threshold are required for the number of physical qubits per logical qubit to remain reasonable [1, 2, 4]. The speed of the operations is also an important parameter: gate speed does not need to be fast in absolute terms (a quantum computer derives its power from the exponential scaling of its workspace with the number of qubits, not from its clock speed), but should be sufficiently fast relative to the qubit coherence time that the memory error is also well below the threshold. In general, there is a trade-off between speed and fidelity, both for specific systems (as studied here) and between different platforms. For example, the strong interactions in the solid state permit sub-microsecond two-qubit gates for superconducting qubits, much faster than is typical for trapped ions, but at present also limit qubit coherence times to $\sim 100\,\mu$s. In both these physical systems, the present limitations to gate speed and fidelity are technical rather than fundamental.

The first detailed proposals for implementing the theoretical ideas of quantum information processing appeared in the 1990s, and were based on laser-cooled trapped ions [11–13], and on single-electron quantum dots [14]. Individual trapped ions possess extremely stable internal states for the storage of quantum information (such states form the basis of some of the most accurate atomic clocks [15]) and the ion-ion coupling arising from the mutual Coulomb repulsion provides a natural mechanism for implementing multi-qubit quantum logic. As in other physical systems, the quantum logic operations which entangle distinct qubits are the most technically challenging to implement, because — however stable the internal qubit states — the quantum information needs to be transmitted between qubits via an external channel which is generally more susceptible to environmental noise. In the case of trapped ions, this channel is the quantized motion of the ions in the harmonic oscillator potential of the trap and is thus sensitive to the effective motional temperature of the ions and to noise in the electric fields used to confine them. The highest fidelity previously reported [9] for a two-qubit gate in trapped ions was 99.3(1)% (a level which has recently been equalled using superconducting qubits [10]); this used an optical qubit transition and hence required good frequency stability in the optical domain. Qubits based on hyperfine ground states, in common with superconducting qubits, operate in the more convenient microwave domain; in contrast to manufactured solid state qubits, however, the qubit frequency is defined by universal atomic properties and this may simplify large-scale architectures.

We report in this Letter an experimental and theoretical study of a two-qubit gate operation [16] for hyperfine trapped-ion qubits driven by Raman laser beams which, together with microwave-driven single-qubit operations, produces a Bell state (a maximally-entangled state) whose fidelity we measure by quantum state tomography. By independent characterization of the single-qubit errors, we infer the error in the gate operation itself. We develop a theoretical error model for the gate, verify the dominant error contributions in auxiliary experiments, and find good agreement with the experimental results. This both confirms the accuracy of our fidelity result, and shows where future work should be focussed. We also measure the average error in laser-driven single-qubit rotations, using randomized benchmarking. For both the single- and two-qubit gates we systematically explore the trade-off between gate speed and error.

The particular two-qubit gate we apply is a $\sigma_z \otimes \sigma_z$ phase gate [16] (σ_z being the Pauli operator), driven by a pair of Raman laser beams at a mean detuning Δ from an optical atomic resonance, where the qubits are stored in the $|\Downarrow\rangle = 4S_{1/2}^{4,+4}$ and $|\Uparrow\rangle = 4S_{1/2}^{3,+3}$ states of the ground hyperfine manifold of $^{43}Ca^+$ (where the superscripts denote the quantum numbers F, M_F; see figure 1a). The

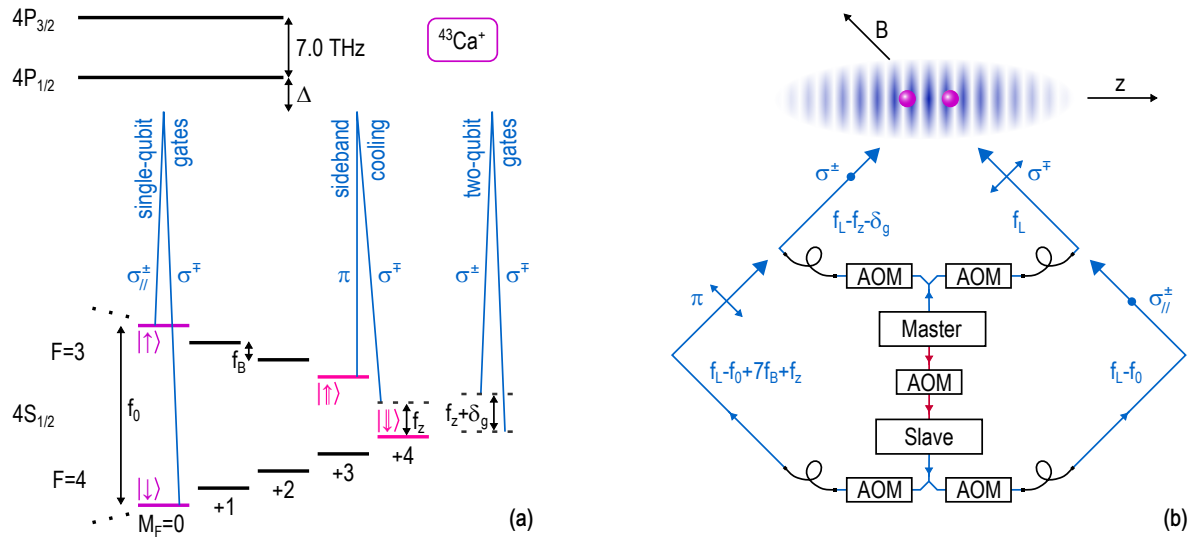

FIG. 1: (a) $^{43}Ca^+$ qubit states and Raman transitions used for sideband cooling, single-qubit and two-qubit gates. The quantization axis is set by a magnetic field $B = 0.196\,\mathrm{mT}$, giving Zeeman splittings $f_B \approx 0.686\,\mathrm{MHz}$ between adjacent hyperfine states. Raman beams have mean detuning $\Delta \sim -1\,\mathrm{THz}$ from the $4S_{1/2} \leftrightarrow 4P_{1/2}$ (397 nm) transition. For single-qubit gates, the Raman difference frequency $\delta = f_0$ where $f_0 = 3.226\,\mathrm{GHz}$ is the $(|\downarrow\rangle,|\uparrow\rangle)$ qubit transition frequency. For sideband cooling, $\delta = f_0 - 7f_B - f_z$ to cool the axial centre-of-mass motion at $f_z = 1.95\,\mathrm{MHz}$, and $\delta = f_0 - 7f_B - f_z\sqrt{3}$ to cool the stretch motion. For two-qubit gates, using the $(|\Downarrow\rangle,|\Uparrow\rangle)$ states, $\delta = f_z + \delta_g$ where $\delta_g = 2/t_g$ with t_g the total gate duration. Global single-qubit $\pi/2$ and π rotations used to characterize the two-qubit gate are driven by microwave radiation. (b) Raman laser system and beam geometry, with the polarizations and frequencies of each beam. The ion separation ($3.5\,\mu$m) is set to be $12\frac{1}{2}$ wavelengths of the travelling standing wave which results from the interference of the two-qubit gate beams. All beams are derived from a master/slave pair of frequency-doubled lasers whose frequency difference ($\approx f_0$) is set by optical injection locking (at 794 nm) via an acousto-optic modulator (AOM) [17]. The beams are frequency-shifted and switched by further AOMs and brought close to the trap using optical fibres. Beam powers are independently stabilized by feedback to the AOMs' r.f. amplitudes. The gate beams are steered onto the ions via mirrors with piezo-electric actuators.

Raman beams exert a state-dependent force on the ions, which transiently excites their centre-of-mass axial motion when they are in the $|\Downarrow\Uparrow\rangle$ or $|\Uparrow\Downarrow\rangle$ states, in turn giving an overall phase on the two-qubit wavefunction for these two states. To vary the gate time t_g we adjust Δ while holding the Raman beam intensity constant; smaller Δ enables a faster gate, at the cost of increased error due to photon scattering [18]. The Raman difference frequency is $\delta = f_z + \delta_g$ where $\delta_g = 2/t_g$ and the axial trap frequency is $f_z = 1.95\,\mathrm{MHz}$. The Raman beams propagate at 45° to the trap z-axis, such that their wavevector difference lies along z (figure 1b). We cool both of the ions' axial modes close to the ground state of motion (mean vibrational quantum number $\bar{n} \approx 0.02$) by Raman sideband cooling; the centre-of-mass mode (with effective temperature $\approx 2\,\mu\mathrm{K}$), rather than the stretch mode, is used to implement the gate to avoid coupling to the hotter ($\sim 1\,\mathrm{mK}$) radial modes of motion [19]. The Raman pulses used to implement the gate are shaped in time, to reduce errors due to off-resonant excitation [20].

We divide the gate operation into two pulses, each of duration $1/\delta_g$, embedded within a global spin-echo sequence [21], which ideally produces the Bell state $|\psi_+\rangle = (|\Downarrow\Downarrow\rangle + |\Uparrow\Uparrow\rangle)/\sqrt{2}$, and use further single-qubit $\pi/2$ rotations to measure the fidelity $F = \langle\psi_+|\rho|\psi_+\rangle$ of the state ρ obtained [16], see figure 2a. Thus the measured Bell state infidelity includes both the error ϵ_g due to the gate operation itself and errors in the single-qubit operations (principally spin-echo ϵ_{SE}, state preparation and measurement ϵ_{SPAM}). We characterize the single-qubit errors by independent experiments in order to extract the two-qubit gate error; the errors in the single-qubit operations are comparable to or smaller than the gate error over the parameter regime studied [20]. The time-dependent dynamics of the gate operation are in excellent agreement with theory (figure 2b).

Results for the complete two-qubit gate data set are shown in figure 3a, where we have normalized throughout for the independently-measured qubit SPAM errors ($\epsilon_{\mathrm{SPAM}} = 1.7 \times 10^{-3}$ per qubit) and spin-echo error ($\epsilon_{\mathrm{SE}} \leq 1.8 \times 10^{-3}$). The data are compared with a theoretical model comprising the four leading sources of gate error [20]. The model gives a minimum error estimate since it assumes all control parameters (for example, laser beam intensities) are set to their optimum values; in reality fluctuations in these parameters, and the finite precision with which each can be set, lead to higher errors. Despite this, the data exceed the model prediction by, on average, less than a factor of two over the full range of gate speeds studied. The lowest gate error is found

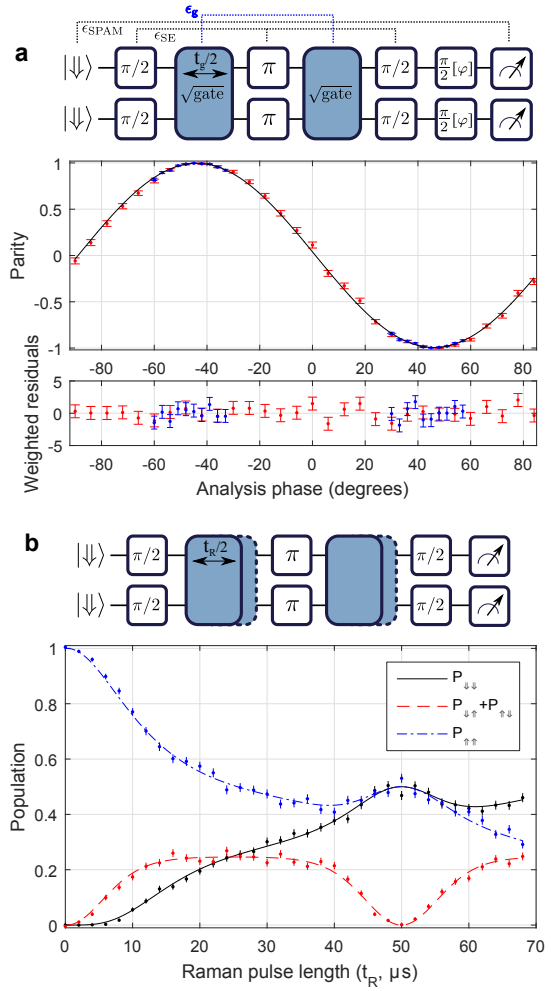

FIG. 2: (a) Quantum state tomography for the optimum two-qubit gate obtained ($t_g = 100\,\mu$s). Parity signal ($P_{\Downarrow\Downarrow} + P_{\Uparrow\Uparrow} - P_{\Downarrow\Uparrow} - P_{\Uparrow\Downarrow}$ where P_α is the probability of finding the ions in state $|\alpha\rangle$), obtained by analysing the Bell state with $\frac{\pi}{2}[\phi]$ tomography pulses whose phase ϕ is scanned relative to that of the single-qubit spin-echo pulses. The operation sequence is shown above, with the sources of the different contributions ϵ to the measured Bell state error indicated. Two independent runs are plotted (red: 1000 sequences per point, blue: 2000 sequences per point). The curve is the maximum likelihood fit to the data [20]; the weighted residuals are shown below, and give a reduced $\chi^2 = 0.87$. (b) Population dynamics during the gate operation, obtained by scanning the duration t_R of the Raman laser pulses, as illustrated above. The Bell state is generated at $t_R = t_g = 50\,\mu$s here. For pulse durations not equal to integer multiples of $1/\delta_g$ the ions' motion does not return to its initial state, which requires the phase of the force to be synchronized between the two Raman pulses. The curves show the ideal gate dynamics with no free parameters except t_g. Error bars in both plots show 1σ statistical errors, calculated using binomial statistics.

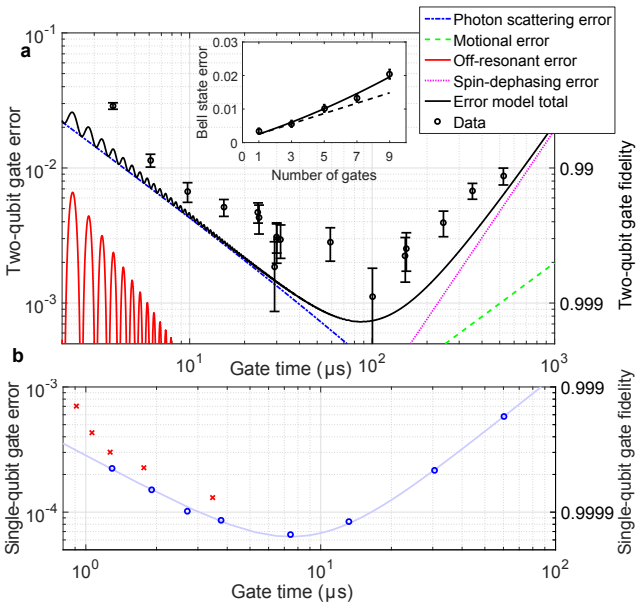

FIG. 3: (a) Measured two-qubit gate error (circles) and error model (lines), plotted against the two-qubit gate duration t_g which was varied by adjusting the Raman detuning Δ at constant Raman beam power. Single-qubit SPAM and spin-echo errors have been subtracted from the data to allow comparison with the error model (see text). The four largest error contributions are plotted, with their total (black line). Inset: Bell state error vs number of two-qubit gates, using $t_g = 30\,\mu$s. The dashed line is the error model prediction of 1.5×10^{-3} per gate, while the solid line is a quadratic fit allowing for a systematic error in the Raman beam intensity of 0.5% (consistent with the observed level of drift [20]). (b) Measured single-qubit gate error versus gate time $t_{\pi/2}$. The minimum error of $0.066(3)\times10^{-3}$ is achieved at $t_{\pi/2} = 7.5\,\mu$s, at which point the contribution to the error from photon scattering is calculated to be 0.02×10^{-3}. Here the gate duration was changed by adjusting the Raman beam intensity; two fixed detunings were used, $\Delta = -1.9\,$THz (circles) and $\Delta = -1.0\,$THz (crosses). Statistical error is smaller than the symbol size. The curve is an empirical model fitted to the data, which allows for differential phase noise between the two Raman beams [20].

at $t_g = 100\,\mu$s (using $\Delta = -3.0\,$THz), where the measured Bell state infidelity is $(1-F) = 2.5(7)\times10^{-3}$ after correcting for SPAM error. For this run, the single-qubit spin-echo error contribution is $\epsilon_{\rm SE} = 1.4(1)\times10^{-3}$, and we infer a gate error of $\epsilon_g = 1.1(7)\times10^{-3}$, representing more than an order of magnitude improvement compared with that previously reported for hyperfine qubits [16, 22, 23]. The measured gate error is consistent with the calculated contributions to ϵ_g given in table I. The shortest gate time attempted was $t_g = 3.8\,\mu$s, for which we measure an error $\epsilon_g = 29(2)\times10^{-3}$; this is a five-fold increase in gate speed, and a factor two reduction in error, compared with the fastest previous trapped-ion implementation [24].

We also performed multiple $t_g = 30\,\mu$s gates within a single, fixed-length, spin-echo sequence (figure 3a, inset); as $\epsilon_{\rm SE}$ and $\epsilon_{\rm SPAM}$ do not vary with the number of gates, this allows an independent estimate of the two-qubit gate error. Making the conservative assumption of an error linear in the number of gates, we obtain an error-per-

two-qubit gate error source (at $t_g = 100\,\mu$s, $\Delta = -3.0\,$THz)	calculated error $/10^{-3}$
Raman+Rayleigh photon scattering	0.4
motional heating and dephasing	0.2
spin dephasing	0.2
Raman beam intensity drift ($< 0.5\%$)	< 0.06
motional temperature ($\bar{n} < 0.05$)	< 0.04
off-resonant effects	< 0.01
total	0.9

TABLE I: Dominant contributions to the two-qubit gate error ϵ_g, as predicted by our theoretical error model for the conditions under which we measured the lowest gate error $\epsilon_g = 1.1(7)\times10^{-3}$. The uncertainty is at most ±1 in the final digit. For details of the calculations, see [20] and [25].

gate of $\epsilon_g = 2.0(2)\times10^{-3}$, independent of all single-qubit and SPAM errors; this value of ϵ_g is dominated by the calculated increase in photon scattering error compared with the $100\,\mu$s gate. It would be desirable to perform longer sequences of gates, for example for the purpose of randomized benchmarking [24]; however, in our system this would not yield useful information on the two-qubit gate error, as the measured error would be dominated by single-qubit errors, due to the effects of 50 Hz magnetic field noise and the magnetic field offset between the two ions [20].

To test the performance of single-qubit gates ($\pi/2$ rotations) driven by the same Raman laser system, we used instead the qubit states $|\downarrow\rangle = 4\mathrm{S}^{4,\,0}_{1/2}$ and $|\uparrow\rangle = 4\mathrm{S}^{3,\,0}_{1/2}$. These states are nearly independent of magnetic field to first order, allowing randomized benchmarking [26] to be used (which is necessary to render the gate error observable above the state preparation and measurement errors). The two-qubit gate cannot be directly applied to these "memory qubit" states [27], but mapping between similar memory and gate qubits in ^{43}Ca$^+$ has been demonstrated with error 0.2×10^{-3} using microwave techniques [28]; mapping both ways for two qubits would thus increase the net two-qubit gate error, but this additional mapping cost should be straightforward to reduce by improved magnetic field control. We employed the same randomized benchmarking protocol as in previous work on microwave-driven single-qubit gates [28], here using typically 160 distinct random sequences each consisting of up to 1000 computational gates. Results are shown in figure 3b; the average gate error is below 1×10^{-3} over the entire range of gate speeds studied ($0.9\,\mu\mathrm{s}\ldots60\,\mu\mathrm{s}$), with a minimum of $0.066(3)\times10^{-3}$ at a gate duration of $t_{\pi/2} = 7.5\,\mu$s. This represents a five-fold reduction in error compared with previous laser-driven single-qubit gates, without incurring the overhead of composite pulse techniques [29]. For a pair of ions, we also demonstrated individual qubit addressing using the trap's axial micromotion [30] with an estimated cross-talk error of $0.1(1)\times10^{-3}$ [20].

We now discuss the prospects for implementing the single- and two-qubit laser gates described in the present work in ion trap systems suitable for scalable quantum information processing, without sacrificing gate fidelity. Two complementary schemes are currently being pursued, the "quantum CCD" approach in which ions are shuttled around a large microfabricated array of interconnected traps [13] and a "network" model where multiple small traps are connected by photonic links which enable heralded entanglement [31]. Both schemes require local deterministic gates with errors $\ll 1\%$ [32]. Sympathetic cooling using a different ion species will also be necessary [13]; we have previously used ^{40}Ca$^+$ for this purpose [33], and have recently demonstrated that the two-qubit gate used here is also capable of mapping quantum information coherently between these two isotopes [34]. For improved protection of logic qubits different elements can be used [35]. In the network model, a macroscopic ion trap such as that used in this work could be used at each node of the network, although it would be advantageous to have several interconnected trapping zones at each node [32]. In the quantum CCD model, microfabricated surface-electrode traps are likely to be necessary because of the large number of zones required [36].

The first difficulty in using surface traps is that the ions are typically trapped much closer to the electrodes, where the electric field noise is greater, disrupting the coherent motional dynamics of the gate. For example, in the room-temperature surface trap used for the high-fidelity single-qubit work reported in [28], we have measured motional heating and decoherence rates one to two orders of magnitude higher than in the macroscopic trap used here. According to our error model, this will limit the two-qubit gate error to a minimum of $\epsilon_g \approx 1\times10^{-3}$. However, significant reductions in electric field noise have been obtained in surface traps, either by cooling the electrodes to cryogenic temperatures [37] or by *in situ* cleaning of the electrode surfaces [38, 39]; this should allow significantly lower ϵ_g. A second technical issue for surface traps is the proximity of the relatively powerful Raman beams to the surface: stray laser light can cause charging of the trap [40], which also leads to uncontrolled electric fields. We have investigated this by aligning a beam of similar power to our Raman beams on an ion trapped $75\,\mu$m above the surface trap used in [28]; we find no detectable change in the required compensation field, at a level $\approx 1\,$V/m, indicating that for light of the wavelength (397 nm) required for ^{43}Ca$^+$, and these trap materials (gold electrodes on a sapphire substrate), charging is not a significant problem and there would be negligible effect on the gate error.

All the contributions to the two-qubit gate error budget (Table I) can be reduced by technical improvements; for example, improved magnetic field stabilization would reduce the spin dephasing error. The only error which is

fundamentally limited is that due to photon scattering; this can be reduced to the $\approx 0.1 \times 10^{-3}$ level (in $^{43}Ca^{+}$) by a factor ≈ 5 increase in the Raman beam intensity [18, 25]. The laser power used in these experiments is modest (5 mW in each gate beam, with waist 27 μm), and could be further reduced by integrating optical elements with the trap structure, allowing more tightly focussed beams while retaining beam-pointing stability [41]. Solid state diode lasers are a more readily scalable technology than the frequency-doubled lasers used in this work, and it has been shown that similar power and spectral purity can be obtained from the latest generation of violet laser diodes, using optical injection locking [42]; an array of such injected diodes could be used to implement thousands of gate operations in parallel. We conclude that, with existing technology, the 99.9% two-qubit gate fidelity demonstrated here can be maintained and improved in the ion trap systems currently envisaged for the implementation of large-scale quantum computation. The task of scaling up quantum information processors beyond the present generation of few-qubit demonstrators remains a formidable one, but we hope that this work will both enable and stimulate efforts to address this technical challenge.

We note that laser-driven quantum logic gates with comparable fidelity have recently been reported by the NIST Ion Storage Group, using $^{9}Be^{+}$ hyperfine qubits [43].

We thank other members of the Oxford ion trap group, especially D. N. Stacey and A. M. Steane, for their contributions to these experiments and for comments on the manuscript. We are grateful to D. T. C. Allcock, S. C. Benjamin, J. P. Home, D. Leibfried, R. Ozeri, T. R. Tan and D. J. Wineland for helpful discussions, and to the ETH Trapped Ion Quantum Information group for the development of direct digital synthesis hardware. This work was supported by the U.K. EPSRC "Networked Quantum Information Technology" Hub and the U.S. Army Research Office (ref. W911NF-14-1-0217).

* Electronic address: d.lucas@physics.ox.ac.uk

[1] A. M. Steane, Phys.Rev.A**68**, 042322 (2003).
[2] E. Knill, Nature **434**, 39 (2005).
[3] R. Raussendorf, J. Harrington, and K. Goyal, New J.Phys. **9**, 199 (2007).
[4] A. G. Fowler *et al.*, Phys.Rev.A**86**, 032324 (2012).
[5] Q. A. Turchette *et al.*, Phys.Rev.Lett. **81**, 3631 (1998).
[6] M. Steffen *et al.*, Science **313**, 1423 (2006).
[7] L. Isenhower *et al.*, Phys.Rev.Lett. **104**, 010503 (2010).
[8] M. Veldhorst *et al.*, Nature **526**, 410 (2015).
[9] J. Benhelm *et al.*, Nat.Phys. **4**, 463 (2008).
[10] R. Barends *et al.*, Nature **508**, 500 (2014).
[11] J. I. Cirac and P. Zoller, Phys.Rev.Lett. **74**, 4091 (1995).
[12] A. M. Steane, App.Phys.B**642**, 623 (1997).
[13] D. J. Wineland *et al.*, J.Res.NIST **103**, 259 (1998).
[14] D. Loss and D.P.DiVincenzo, Phys.Rev.A**57**, 120 (1998).
[15] A. D. Ludlow *et al.*, Rev.Mod.Phys. **87**, 637 (2015).
[16] D. Leibfried *et al.*, Nature **422**, 412 (2003).
[17] N. M. Linke, C. J. Ballance, and D. M. Lucas, Opt.Lett. **38**, 5087 (2013).
[18] R. Ozeri *et al.*, Phys.Rev.A**75**, 042329 (2007).
[19] C. F. Roos *et al.*, Phys.Rev.A**77**, 040302 (2008).
[20] See Supplemental Material, which includes refs. [44–56], for further details.
[21] J. P. Home *et al.*, New J.Phys. **8**, 188 (2006).
[22] G. Kirchmair *et al.*, Phys.Rev.A **79**, 020304(R) (2009).
[23] T. R. Tan *et al.*, Phys.Rev.Lett. **110**, 263002 (2013).
[24] J. P. Gaebler *et al.*, Phys.Rev.Lett. **108**, 260503 (2012).
[25] C. J. Ballance, Ph.D. thesis, University of Oxford (2014). http://ora.ox.ac.uk/objects/uuid:1beb7f67-4d92-4d57-8754-50f92f9d27f4/
[26] E. Knill *et al.*, Phys.Rev.A**77**, 012307 (2008).
[27] P. Lee *et al.*, J.Opt.B**7**, S371 (2005).
[28] T. P. Harty *et al.*, Phys.Rev.Lett. **113**, 220501 (2014).
[29] E. Mount *et al.*, Phys.Rev.A**92**, 060301(R) (2015).
[30] N. Navon *et al.*, Phys.Rev.Lett. **111**, 073001 (2013).
[31] C. Monroe *et al.*, Phys.Rev.A**89**, 022317 (2014).
[32] N. H. Nickerson, J. F. Fitzsimons, and S. C. Benjamin, Phys.Rev.X**4**, 041041 (2014).
[33] J. P. Home *et al.*, Phys.Rev.A**79**, 050305 (2009).
[34] C. J. Ballance *et al.*, Nature **528**, 384 (2015).
[35] T. R. Tan *et al.*, Nature **528**, 380 (2015).
[36] J. M. Amini *et al.*, New J.Phys. **12**, 033031 (2010).
[37] J. Labaziewicz *et al.*, Phys.Rev.Lett. **100**, 013001 (2008).
[38] D. T. C. Allcock *et al.*, New J.Phys. **13**, 123023 (2011).
[39] D. A. Hite *et al.*, Phys.Rev.Lett. **109**, 103001 (2012).
[40] M. Harlander *et al.*, New J.Phys. **12**, 093035 (2010).
[41] K. K. Mehta *et al.*, ArXiv (2015), arXiv:1510.05618.
[42] V. M. Schäfer *et al.*, Opt.Lett. **40**, 4265 (2015).
[43] T. R. Tan *et al.*, ArXiv (2016), arXiv:1604.00032.
[44] D. M. Lucas *et al.*, Phys.Rev.A**69**, 012711 (2004).
[45] A. H. Myerson *et al.*, Phys.Rev.Lett. **100**, 200502 (2008).
[46] T. P. Harty, Ph.D. thesis, University of Oxford (2013).
[47] N. M. Linke, Ph.D. thesis, University of Oxford (2012).
[48] C. A. Sackett *et al.*, Nature **404**, 256 (2000).
[49] P. A. Barton *et al.*, Phys.Rev.A**62** 032503 (2000).
[50] W. H. Press *et al.*, *Numerical Recipes in C* (Cambridge University Press, 1992).
[51] H. Uys *et al.*, Phys.Rev.Lett. **105**, 200401 (2010).
[52] R. Ozeri *et al.*, Phys.Rev.Lett. **95**, 030403 (2005).
[53] Q. A. Turchette *et al.*, Phys.Rev.A**62**, 053807 (2000).
[54] A. Sørensen and K. Mølmer, Phys.Rev.Lett.**82**, 1971 (1999).
[55] U. Warring *et al.*, Phys.Rev.Lett. **110**, 173002 (2013).
[56] D. J. Szwer, Ph.D. thesis, University of Oxford (2009).